

## Violent Folding of a Flame Front in a Flame-Acoustic Resonance

Arkady Petchenko,<sup>1</sup> Vitaly Bychkov,<sup>1</sup> V'yacheslav Akkerman,<sup>1,2</sup> and Lars-Erik Eriksson<sup>3</sup>

<sup>1</sup>*Institute of Physics, Umeå University, SE-901 87, Umeå, Sweden*

<sup>2</sup>*Nuclear Safety Institute (IBRAE) of Russian Academy of Sciences, B. Tulsakaya 52, 113191 Moscow, Russia*

<sup>3</sup>*Department of Applied Mechanics, Chalmers University of Technology, 412 96 Göteborg, Sweden*

(Received 21 June 2006; published 19 October 2006)

The first direct numerical simulations of violent flame folding because of the flame-acoustic resonance are performed. Flame propagates in a tube from an open end to a closed one. Acoustic amplitude becomes extremely large when the acoustic mode between the flame and the closed tube end comes in resonance with intrinsic flame oscillations. The acoustic oscillations produce an effective acceleration field at the flame front leading to a strong Rayleigh-Taylor instability during every second half period of the oscillations. The Rayleigh-Taylor instability makes the flame front strongly corrugated with elongated jets of heavy fuel mixture penetrating the burnt gas and even with pockets of unburned matter separated from the flame front.

DOI: [10.1103/PhysRevLett.97.164501](https://doi.org/10.1103/PhysRevLett.97.164501)

PACS numbers: 47.70.Pq, 47.20.Ma

The interaction of premixed flames with acoustic waves is one of the most interesting parts of combustion science and nonlinear physics [1–4]. When burning happens under confinement, flame generates acoustic waves of considerable amplitude. The acoustic waves, in turn, make the flame front more corrugated or smoother, depending on the geometry and flow parameters. Some important aspects of this interaction have been discussed first by Markstein [3] and demonstrated later in the classical experiments by Searby [1]. Particularly, Searby observed that sufficiently fast flames produce extra-strong acoustic waves and lead to violent turbulent burning in the second half of the tube. The experiments by Searby [1] induced a number of theoretical, numerical, and experimental works on the subject [5–12]. However, the important phenomenon of flame turbulization has not been explained so far. Some ideas in that direction have been proposed in [9], but the effects considered in [9] were noticeably weaker than the turbulent burning in the experiments [1].

In the present work we performed the first direct numerical simulations of violent flame folding because of the flame-acoustic resonance. The effects obtained are as strong as the experimental observations in [1,11]; the combustion geometry is also qualitatively similar. We consider a flame propagating in a tube from an open end to a closed one. We solve the complete system of gas-dynamic combustion equations including transport processes and a hypothetical single irreversible Arrhenius reaction of the first order. Because of the limited space, we do not present the equations here, since they are standard and may be found in our previous works [13–15]. The burning substance is a perfect gas with heat capacity  $C_V = 5R_p/2m$ , which does not depend on the reaction ( $R_p$  is the perfect gas constant). We took the initial pressure and temperature of the fuel mixture  $P_f = 10^5$  Pa and  $T_f = 300$  K. We chose chemical parameters to obtain the planar flame velocity  $U_f = 3.47$  m/s, which is 100 times smaller

than the sound speed. The chosen velocity exceeds noticeably the velocity of propane flames, but it is needed to reduce the computational time. Heat release in the burning process leads to gas expansion; we take the density ratio of the fuel mixture and the burnt matter  $\rho_f/\rho_b = 8$  typical for methane and propane burning. The flame thickness is defined in a conventional way as  $L_f \equiv \mu/(\text{Pr}\rho_f U_f)$ , where  $\mu = 2.38 \times 10^{-5}$  Ns/m<sup>2</sup> is the dynamic viscosity and  $\text{Pr} = 0.7$  is the Prandtl number. Still, we stress that  $L_f$  is just a mathematical parameter of length dimension, rather than a real flame thickness. Numerical simulations demonstrate that the real thickness of a flame front exceeds the value  $L_f$  by a factor of 4–5 or even larger [15]. We chose the unit Lewis number  $\text{Le} = 1$  and the activation energy  $E_a = 56R_p T_f$ , which allows smoothing the reaction zone over few computational cells. The numerical method was described in detail in our recent work [15]. We investigated burning in a channel of width  $D$  closed at one end. The flame propagates from the open end to the closed one generating acoustic waves because of the boundary conditions. We considered adiabatic tube walls, which may be nonslip or slip. At the tube end we used either nonreflecting boundary conditions or conditions of constant pressure. In both cases we obtained similar results, which indicates that the principal acoustic mode is of minor importance in the resonance. The most important acoustic mode is that between the flame front and the closed tube end. We chose the  $z$  axis directed along the tube walls, while the  $x$  axis was perpendicular to the walls. To reduce numerical errors and to perform calculations in a reasonable time we used a rectangular grid with the step  $0.2L_f$  in  $z$  direction. In  $x$  direction we used the steps  $0.2L_f$  and  $0.5L_f$ ; in both cases the results were similar. The mesh was uniform all over the tube, since we had to resolve not only the flame structure, but also the acoustic waves. In the previous paper [15] we have tested the computational accuracy of a similar prob-

lem using even finer mesh, with twice smaller cells, and found good agreement of the results obtained for the fine and coarser grid.

We performed the simulations for different tube widths within the domain  $10 < D/L_f < 60$  and for the tube lengths  $20 < L/D < 100$ . In this Letter we discuss the simulation runs for  $D = 35L_f$ ,  $L = 40D$ , which demonstrate violent flame folding clearly. Other simulation results will be analyzed in detail elsewhere. Of course, the tube width and length considered in the simulations are much smaller than any realistic tube width or length. Small length scales are a usual limitation for direct numerical simulations with reasonable resolution of the flame structure. An initially planar flame front was placed close to the open tube end (at the distance  $100L_f$  from the end). Initially, the fuel mixture was at rest,  $\rho = \rho_f$ ,  $T = T_f$ ,  $u_z = 0$ ,  $u_x = 0$ , while the gas expansion in the burning process induced a flow of burnt matter out of the tube. Since gas cannot move along the nonslip walls, then we obtain a nonuniform velocity profile in the burnt gas leading to a curved flame shape shown in Fig. 1. According to [15], in a tube of width  $D = 35L_f$  with both ends open one should expect flame oscillations with the average velocity about  $1.5U_f$ , with the oscillation amplitude about  $U_f$  and with the period about  $(0.5-1)\tau$ , where  $\tau = D/U_f$ . At the beginning of the present simulations we observed a similar picture. However, in the present case, flame oscillations generate an acoustic wave in the limited space between the closed tube end and the flame front. Flame-acoustic interaction eventually makes the oscillations stronger. Figure 1 presents the initial stage of flame dynamics, which demonstrates clearly an increase of the oscillation amplitude in time. We observed similar oscillations even in narrow tubes  $D/L_f = 10-20$ , for which Ref. [15] demonstrated the stationary flame propagation. Still, the simulation runs for narrow tubes show flame oscillations of moderate amplitude, and they are not presented here. Violent flame folding was observed only for tubes with  $D > 25L_f$ . As the flame approaches the closed tube end, the oscillation amplitude increases. Figure 2 shows representative flame shapes at the time instants  $t/\tau = 6.71; 6.75; 6.77$ . In spite of a rather small tube width (which implies considerable smoothing influence of thermal conduction), the flame front is strongly corrugated. In Fig. 2(a) we can see an elongated jet of the fuel mixture developing at the flame front. In Fig. 2(b), most of the jet is separated from the main flame front by a ‘‘bottleneck’’. Finally, the jet col-

lapses in Fig. 2(c) pushing a blob of burnt matter into the fuel mixture. Flame structure in Fig. 2(c) looks quite similar to the experimental photo in Fig. 6a of Ref. [1]. Time variations of the total flame length scaled by the tube width  $D_w/D$  are shown in Fig. 3. The plot demonstrates clearly an increase of the oscillation amplitude in time. The total flame length in the oscillations may exceed the planar flame length by the factor of  $D_w/D = 35$ . The oscillation period varies slightly during the simulation run  $\tau_p/\tau = 0.3-0.37$ . This period is comparable to the values obtained for flame oscillations in open tubes of similar width, with influence of acoustic waves eliminated by the nonreflecting boundary conditions [15]. The oscillation period is, presumably, an intrinsic parameter of flame dynamics in a tube with nonslip walls. Modifications of the period with changing oscillation amplitude may happen because of nonlinear effects [16]. Figure 4 shows oscillations of  $z$ -velocity component in the acoustic wave ahead of the flame front, which may be as large as  $U_a \approx 63U_f$ . The reason for such a large acoustic amplitude is a resonance between the flame oscillations and the acoustic mode. We calculate the acoustic period  $\tau_a$  as the time needed for sound to travel from the flame front to the closed tube end and back. Considerable increase of the oscillation amplitude starts when the acoustic period becomes about the pulsation period,  $\tau_p/\tau_a \approx 1$ ; at that point amplitude of flame oscillations reaches  $D_w \approx 16D$ . Presumably, time is needed to excite strong acoustic waves, because maximal flame amplitudes are observed little later, when  $\tau_p/\tau_a \approx 0.5$ . However, at the very end of the tube, the resonance condition does not hold any more and the oscillation amplitude goes down quite fast. Taking slip boundary conditions at the walls (instead of nonslip) we did not obtain flame oscillations and any sign of a resonance. Instead, the flame acquired a quasistationary shape typical for the nonlinear stage of the Darrieus-Landau instability in tubes of moderate widths [13,17,18].

Another question concerns the physical nature of violent flame folding. The elongated jet of heavy fuel mixture in Fig. 2(a) resembles the Rayleigh-Taylor (RT) instability at the nonlinear stage. We remind that the RT instability develops at an interface between the heavy and light matter in a gravitational field. The nonlinear stage of the instability is typically described as large bubbles of light gas rising up and jets of the heavy gas falling down similar to the flow of Fig. 2(a); see [13,19–22]. In order to check the possibility, we have to understand the role of a time-

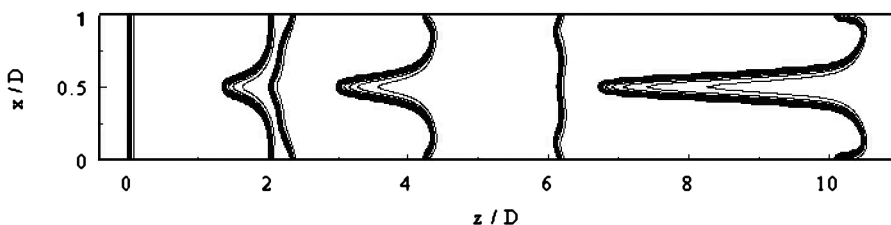


FIG. 1. Flame shape at the time instants  $t/\tau = 0; 0.86; 1.04; 1.81; 2.46; 3.51$  shown by isotherms (400–2200 K with step 200 K).

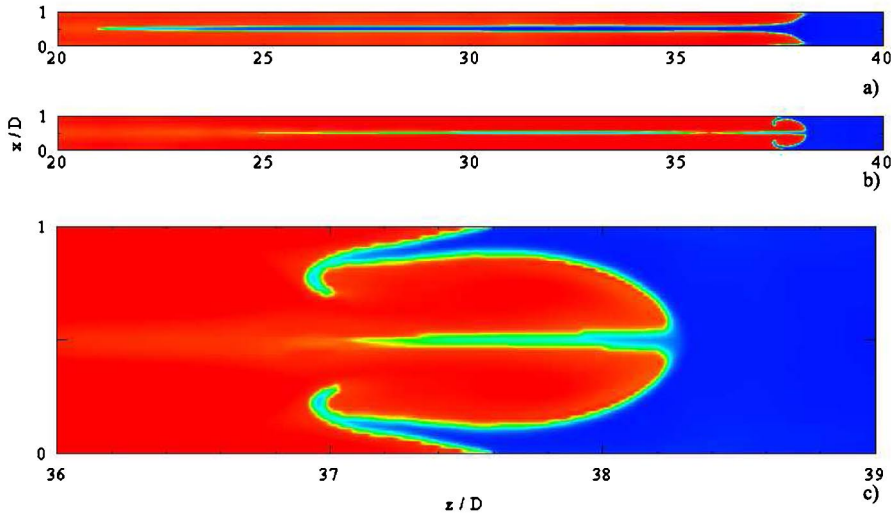


FIG. 2 (color online). Flame shape at the time instants  $t/\tau = 6.71$ ;  $6.75$ ;  $6.77$  [(a), (b), (c), respectively] shown by colors (blue corresponds to 300 K of the fuel mixture and red corresponds to 2400 K of the burnt matter).

dependent acceleration produced by the acoustic wave. The acceleration may be evaluated as  $\omega_a U_a$ , where  $\omega_a = 2\pi/\tau_a$  is the acoustic frequency. The acceleration role is characterized by the inverse Froude number

$$\frac{gD}{U_f^2} = \tau \omega_a \frac{U_a}{U_f} = 2\pi \frac{\tau}{\tau_a} \frac{U_a}{U_f}. \quad (1)$$

Substituting characteristic values  $U_a \approx 60U_f$ ,  $\tau_a \approx \tau_p \approx 0.3\tau$  into Eq. (1) we obtain the inverse Froude number  $gD/U_f^2 \approx 10^3$ . Of course, such a huge acceleration leads to a strong RT instability. Besides, one has to check if the instability has sufficient time to develop. For that purpose we compare the characteristic growth rate of the RT instability  $\sqrt{gk} = \sqrt{2\pi g/D}$  to the inverse half period of the flame pulsations  $\tau_p/2$ , during which the oscillating acceleration plays a destabilizing role

$$\frac{1}{2}\sqrt{gk}\tau_p = \pi\sqrt{\frac{U_a}{\tau_a D}}\tau_p \approx \pi\sqrt{\frac{U_a\tau_p^2}{U_f\tau_a\tau}}. \quad (2)$$

Evaluating the above parameter, we find  $\sqrt{gk}\tau_p/2 \approx 14$ , which indicates that half period of the flame oscillations is quite sufficient for the strong RT instability to arise. In the other half period the acceleration changes sign, becomes stabilizing, and the elongated jet of Fig. 2(a) collapses fast because of the flame propagation. This collapse is even accompanied by a blob of burnt matter pushed into the fuel mixture. The inversion of the flame shape (from strongly concave to convex) is similar to the Richtmyer-Meshkov instability [3,23–27], which occurs at an interface of density drop hit by a shock wave. The described process satisfies also the Rayleigh criterion: flame becomes more corrugated when pressure increases in the acoustic wave [2]. Besides, the Reynolds number for the flow may be evaluated as  $Re = U_a D / \text{Pr} U_f L_f = (2-3) \times 10^3$ , which is

comparable to the critical value of  $Re$  for transition to turbulence in tubes.

Finally, it is interesting to compare the present numerical results to the experiments [1,11]. Similar to the experiments, in the present modeling, violent flame folding is observed close to the tube end. According to [1], the flame velocity may increase by a factor about 18 because of turbulence, which is comparable to the data of Fig. 3. Unfortunately, Searby did not report the velocity amplitude in acoustic oscillations in [1]. This value was measured later by Aldredge and Killingthworth [11] in a similar experiment for methane-air flames. They found the maximal acoustic amplitude about  $(48-54)U_f$ , which is close to the present results. The tube diameter in [1] was 10 cm; the experimental setup in [11] used a flame propagating between two cylinders with the gap of 1.1 cm. Scaled by  $L_f = (5-6) \times 10^{-3}$  cm for stoichiometric methane and propane flames [28], these lengths correspond approximately to  $2 \times 10^3 L_f$  and  $200 L_f$ , respectively. Of course, both scales are much larger than the channel width of the present simulations. By this reason, the role of nonslip

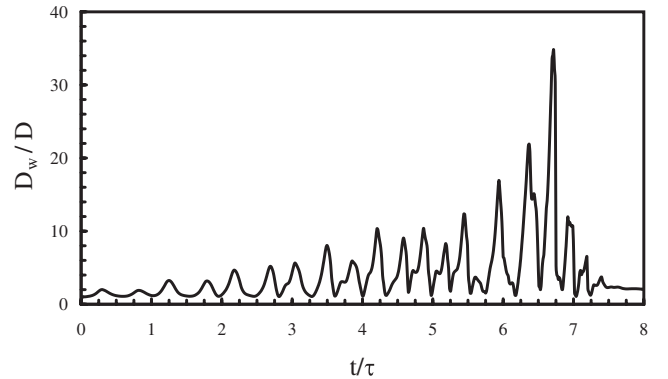


FIG. 3. Time variations of the total flame length scaled by the tube width  $D_w/D$ .

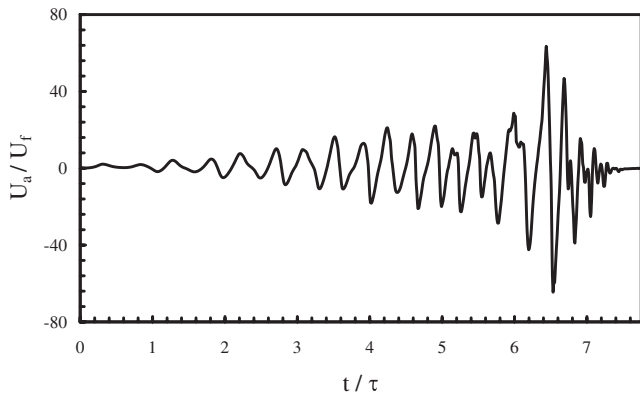


FIG. 4. Time variations of  $z$ -velocity component  $U_a$  in the acoustic wave ahead of the flame front.

walls in the experiments is questionable, since the respective oscillation period depends strongly on the tube width. It is possible that the resonant turbulence observed experimentally involves another type of intrinsic flame oscillations, e.g., due to the parametric flame instability. As a result, extrapolation of the present modeling to the experimental domain is not straightforward.

Thus, the present simulations demonstrate violent folding of a flame front in a flame-acoustic resonance. The effect has many features in common with the experiments [1,11] like extra-large increase of the flame speed and extra-strong acoustic waves. Still, an inevitably limited parameter domain of the simulations does not allow direct quantitative comparison of the present results to the experiments.

The authors are grateful to Mikhail Ivanov for useful discussions. This work has been supported in part by the Swedish Research Council (VR) and by the Kempe Foundation.

- 
- [1] G. Searby, *Combust. Sci. Technol.* **81**, 221 (1992).
  - [2] F. A. Williams, *Combustion Theory* (Benjamin, New York, 1985).
  - [3] G. Markstein, in *Non-Steady Flame Propagation*, edited by G. Markstein (Pergamon, New York, 1964), p. 15.

- [4] Ya. B. Zeldovich, G. I. Barenblatt, V. B. Librovich, and G. M. Makhviladze, *Mathematical Theory of Combustion and Explosion* (Consultants Bureau, New York, 1985).
- [5] G. Searby and D. Rochwerger, *J. Fluid Mech.* **231**, 529 (1991).
- [6] B. Denet and A. Toma, *Combust. Sci. Tech.* **23**, 109 (1995).
- [7] V. Bychkov, *Phys. Fluids* **11**, 3168 (1999).
- [8] V. Vaezi and R. C. Aldredge, *Combust. Flame* **121**, 356 (2000).
- [9] V. Bychkov, *Phys. Rev. Lett.* **89**, 168302 (2002).
- [10] X. Wu, M. Wang, P. Moin, and N. Peters, *J. Fluid Mechanics* **23**, 497 (2003).
- [11] R. C. Aldredge and N. J. Killingsworth, *Combust. Flame* **137**, 178 (2004).
- [12] R. C. Aldredge, *Combust. Sci. Technol.* **177**, 53 (2005).
- [13] V. Bychkov and M. Liberman, *Phys. Rep.* **325**, 115 (2000).
- [14] V. Bychkov, A. Petchenko, V. Akkerman, and L. E. Eriksson, *Phys. Rev. E* **72**, 046307 (2005).
- [15] V. Akkerman, V. Bychkov, A. Petchenko, and L. E. Eriksson, *Combust. Flame* **145**, 675 (2006).
- [16] L. D. Landau and E. M. Lifshitz, *Mechanics* (Pergamon, New York, 1989).
- [17] V. Bychkov, S. Golberg, M. Liberman, and L. E. Eriksson, *Phys. Rev. E* **54**, 3713 (1996).
- [18] O. Travnikov, V. Bychkov, and M. Liberman, *Phys. Rev. E* **61**, 468 (2000).
- [19] H. Kull, *Phys. Rep.* **206**, 197 (1991).
- [20] N. Inogamov and A. Oparin, *J. Exp. Theor. Phys.* **481**, 89 (1999).
- [21] C. Clanet, P. Heraud, and G. Searby, *J. Fluid Mech.* **519**, 359 (2004).
- [22] P. Ramaprabhu and G. Dimonte, *Phys. Rev. E* **71**, 036314 (2005).
- [23] R. D. Richtmeyer, *Commun. Pure Appl. Math.* **13**, 297 (1960).
- [24] E. E. Meshkov, *Fluid. Dyn. (USSR)* **4**, 101 (1969).
- [25] C. Clanet and G. Searby, *Combust. Flame* **105**, 225 (1996).
- [26] V. Bychkov, *Phys. Fluids* **10**, 2669 (1998).
- [27] O. Travnikov, V. Bychkov, and M. Liberman, *Combust. Sci. Techn.* **142**, 1 (1999).
- [28] S. G. Davis, J. Quinard, and G. Searby, *Combust. Flame* **130**, 123 (2002).